A Letters Journal Exploring the Frontiers of Physics

March 2009

EPL, **85** (2009) 67005
doi: 10.1209/0295-5075/85/67005

www.epljournal.org

Magnetic screening in proximity effect Josephson-junction arrays

M. Tesei[1] and R. Théron[2]

[1] *The Blackett Laboratory, Imperial College - London SW7 2BZ, UK, EU*
[2] *Ecole Polytechnique Fédérale de Lausanne (EPFL), Institute of Microengineering IMT, Photovoltaics and thin film electronics laboratory - Neuchâtel, Switzerland*

received 2 July 2008; accepted in final form 2 March 2009
published online 8 April 2009

PACS 74.81.Fa – Josephson junction arrays and wire networks
PACS 74.25.Ha – Magnetic properties
PACS 64.60.De – Statistical mechanics of model systems (Ising model, Potts model, field-theory models, Monte Carlo techniques, etc.)

Abstract – The modulation with magnetic field of the sheet inductance measured on proximity effect Josephson-junction arrays (JJAs) is progressively vanishing on lowering the temperature, leading to a low-temperature field-independent response. This behaviour is consistent with the decrease of the two-dimensional penetration length below the lattice parameter. Low-temperature data are quantitatively compared with theoretical predictions based on the XY model in the absence of thermal fluctuations. The results show that the description of a JJA within the XY model is incomplete and the system is put well beyond the weak screening limit which is usually assumed in order to invoke the well-known frustrated XY model describing classical Josephson-junction arrays.

Introduction. – Proximity effect Josephson-junction arrays (JJAs) exposed to a perpendicular magnetic field B are well known to be, under some conditions discussed below, a good physical realization of the frustrated XY model [1] and so have been studied for many years as model systems, and still reveal some interesting physics [2]. The description of JJAs in the framework of the frustrated XY model remains valid in a broad temperature range below the superconducting-to-normal transition temperature T_c. In the case of proximity effect SNS JJAs, quantum fluctuations are irrelevant even at very low temperature. Indeed, the Josephson coupling energy $E_J = \phi_0 I_c/2\pi$ (ϕ_0 the flux quantum and I_c the single-junction critical current) is much larger than the Coulomb charging energy $E_c = e^{*2}/2C$ ($e^* = 2e$ the free Cooper-pair charge and C the junction capacitance), and the normal-state resistance is much smaller than the quantum resistance [3] (roughly 7 orders of magnitude smaller in our systems). These two criteria ensure that our JJAs remain in the classical regime for all $T < T_c$. However, when lowering the temperature magnetic interactions (between screening currents of neighbouring cells) put the system beyond the pure XY model. As a matter of fact, the system experiences a gradual crossover from a *high-temperature XY weak-screening regime*, where vortex ground states satisfy the fluxoid quantisation in all plaquettes [1], and the local magnetic field equals the applied field B, to a *low-temperature strong-screening regime* with quantised flux where B penetrates the JJA in a similar way to how it penetrates a superconducting wire network creating an Abrikosov-like lattice. In the weak-screening limit, the frustration parameter f is defined by the magnetic flux ϕ threading an elementary cell in units of the flux quantum ϕ_0; $f = \phi/\phi_0$. While lowering the temperature, the JJA is gradually put beyond the weak-screening limit when supercurrents flowing around each lattice cell are no longer negligible. At very low temperatures, when an elementary cell of the array is able to fully screen a flux quantum, any connection to the XY model is lost since the JJA behaves as a multiply connected superconductor.

Although their existence is well known, the effects of screening currents on the behaviour of JJAs have been investigated mainly theoretically, in the weak-screening regime (as a correction of the frustrated XY model) [4] and beyond [5,6]. This paper focuses on the low-temperature regime of JJAs on a periodic lattice with hexagonal symmetry called a *dice* lattice (see fig. 1 and description below) where the measured sheet inductance is independent of B. In this regime, three different phenomena push our JJA beyond the XY model. Firstly, the effective penetration length becomes shorter than the lattice parameter and the magnetic energy associated with screening currents dominates over the Josephson coupling energy as far as the magnetic field response is concerned. Secondly,

thermal fluctuations gradually vanish and vortex mobility is accordingly reduced. Finally, on a smaller size scale, the Josephson penetration length becomes smaller than the size of a Josephson junction which results in a non-unique phase difference across the junction width. All this leads to a low-temperature regime dominated by magnetic-screening effects which efficiently suppress the field modulation of the measured sheet inductance. This scenario is confirmed by comparing low-temperature sheet inductance data with the same quantity calculated within the frustrated XY model in the absence of thermal fluctuations, *i.e.* in the ground states. Thus, when the temperature is lowered JJAs can easily reach a regime where the XY model is not sufficient to describe their behaviour.

In addition, for the first time data taken using the two-coil mutual inductance technique [7], as well as the related data treatment, are confirmed by comparing I_c extracted from inductive measurements with the same quantity measured by a conventional four probe measurement technique.

Measurement technique. – Arrays of proximity effect Pb-Cu-Pb junctions on a *dice* lattice (see upper inset to fig. 1) were probed using a SQUID-operated two-coil mutual-inductance technique [7] that allows for measurements of the screening properties of superconducting wire networks [8], JJAs [2], as well as high-temperature superconducting thin films [9]. Here the macroscopic measured quantity is the inverse sheet inductance L^{-1} (or inverse inductance "per square" [10]) that is inferred from the array's linear sheet conductance [7], and measures the degree of superconducting phase coherence in the sample. The inductive technique has a sensitivity threshold of the order of 10 pH.

For comparisons with theoretical predictions based on the XY model and with samples with different coupling constants, *i.e.* different geometrical parameters, the temperature is scaled according to the thermal energy k_BT and E_J; the so-called *reduced temperature* is $\tau = k_BT/E_J$. At zero field and at temperatures well below T_c the sheet inductance of a regular array $L \propto L_J$ [10] the single-junction inductance, and the numerical factor depends only on the lattice geometry. For the *dice* lattice [11] $L^{-1}(T) = (2/\sqrt{3})L_J^{-1}(T)$ and $L^{-1}(T) = (2/\sqrt{3})(2\pi/\phi_0)I_c(T)$ [12]. Close to T_c, the critical current I_c is extrapolated from low-temperature data [13].

For the first time inductive measurements performed using the two-coil mutual-inductance technique [7], and the successive data treatment, are independently and directly confirmed by comparing the temperature dependence of the single-junction critical current I_c (at zero field) extracted from inductive measurements on a JJA with the same quantity measured by four probe measurements following the procedure detailed in ref. [14] where I_c is defined as the current that produces a maximum in the dynamic resistance ($\mathrm{d}V/\mathrm{d}I$ *vs.* I). Since

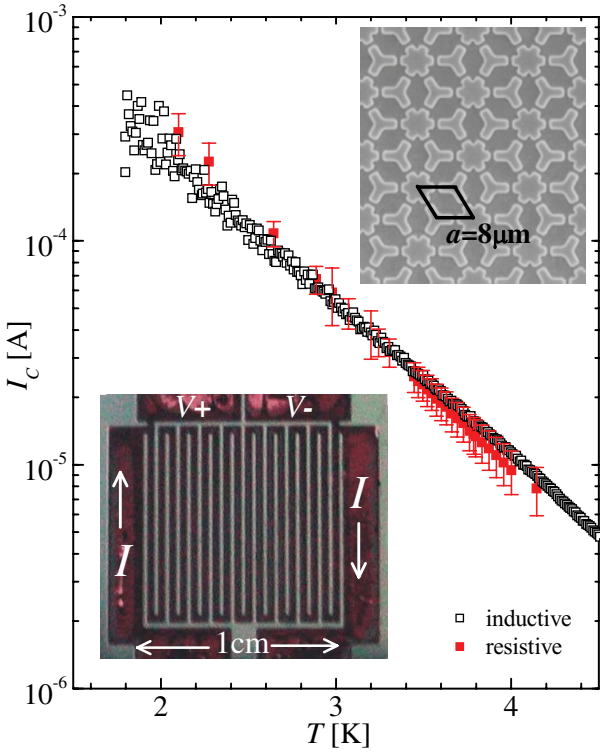

Fig. 1: (Colour on-line) Low-temperature dependence of the single-junction critical current I_c extracted from resistive measurements (red plain symbols) and measured inductively (black empty symbols) at zero field. Upper inset: SEM picture of a portion of a $1 \times 1\,\mathrm{cm}^2$ JJA on *dice* lattice. The array consists of $\sim 10^6$ star-shaped (6-fold and 3-fold) superconducting lead islands coupled by proximity effect junctions in the underlying normal copper layer. The junctions have nominal width $w = 2\,\mu$m and length $l = 1\,\mu$m. An elementary rhombic cell illustrated with black line has a side $a = 8\,\mu$m. Lower inset: photograph taken with an optical microscope of modified sample for resistive $\mathrm{d}V/\mathrm{d}I$ measurements. The current I is injected on copper contacts at bottom into the central zigzag strip, and voltage $V+/V-$ is measured on copper contacts at the top ends of the strip. The strip consists of 18 branches of width about 300 μm containing 48 parallel junctions. The branches are equally spaced by 100 μm and go back and forth across an area slightly smaller than the initial JJA. The strip is about 12 cm long.

the small normal-state sheet resistance of proximity effect JJAs (of the order of a mΩ) and the high current that one would have to apply to approximately 1000 parallel channels of junctions in the $1\mathrm{cm}^2$ sample, and leading to a noticeable increase of temperature in the array, the sample geometry was modified after all inductive measurements were done. A new pattern is obtained by an additional optical lithography process with the photoresist layer spread out on the top of the pre-existing JJA, and part of the superconducting lead islands were removed using Ar-ion milling. The resulting pattern was a thin (48 parallel junctions) and 12 cm long back-and-forth strip across the initial array, as shown in the lower inset

of fig. 1. The pre-existing copper layer all around the JJA is left on the substrate and used for current and voltage contacts, as well as to dissipate the heat due to the measurement current (not shown in fig. 1). This new pattern allows for a lower applied current and the measured voltage drop across the strip is much greater than it would be across the initial array. Particular care during the modification process was taken to avoid residual lead islands in-between the branches of the strip that could create electric shortcuts between the branches. Figure 1 shows low-temperature values of I_c obtained from both inductive measurements on the original JJA and resistive measurements on the modified sample. The error in I_c obtained by resistive measurements is due to the resolution in measuring the current and the related position of the maximum in $\mathrm{d}V/\mathrm{d}I$. The measurements are limited to temperatures below 4.2 K because the sample was immersed in the helium bath of the cryostat to avoid local heating of the junctions which could be induced by the applied current. Insight into the effects of the reduction in the size of the array can be provided by a comparison of our experimental conditions with previous results obtained by numerical simulations of the resistively shunted Josephson-junction model at zero temperature ($T=0$) [5], thus neglecting finite-temperature effects. At zero field and at $T=0$ the dynamics of a JJA reduces to that of a set of uncoupled channels of single junctions along the current direction [5]. In our experiments the ambient magnetic field is reduced by a combination of mu-metal and superconducting screens and at nominally zero field the residual frustration is $f=10^{-3}$ ($B\cong 0.4\,\mathrm{mG}$), which we can reasonably assume small enough to compare our data with results at $f=0$ [5]. A frustration parameter $f=1$, *i.e.* one quantum of flux per cell, is achieved with a perpendicular magnetic field $B\cong 360\,\mathrm{mG}$. When edge fields induced by the applied external current are taken into account and in the case of a 32×32 array [4] (compared to our modified sample with 48 parallel junctions), I_c is reduced by less than 10% when the field penetration length is of the order of the lattice parameter, *i.e.* in the strong screening regime (see discussion below). In the following we show that in our JJAs such a strong screening regime is achieved for temperatures $T<3\,\mathrm{K}$. Thus we do not expect our resistive measurements to be significantly affected by the reduced size of the sample, except possibly for the few measurements below 3 K in fig. 1. The data presented in fig. 1 show the validity of the measurement technique, as well as the procedure to extract the critical current.

Results and discussion. – In the weak-screening regime, due to the nature of the coupling in JJAs [1], the frustration f can induce a pronounced modulation of the single-junction inductance $L_J(T)=(\phi_0/2\pi)/(I_c(T)\cos(\theta))$ [15], hence the measured sheet inductance $L(T)$, where θ is the gauge-invariant phase difference related to f by the fluxoid quantisation [1,2]. Figure 2 shows the response of a JJA while sweeping B in the reduced interval $0<f<1/2$ [1].

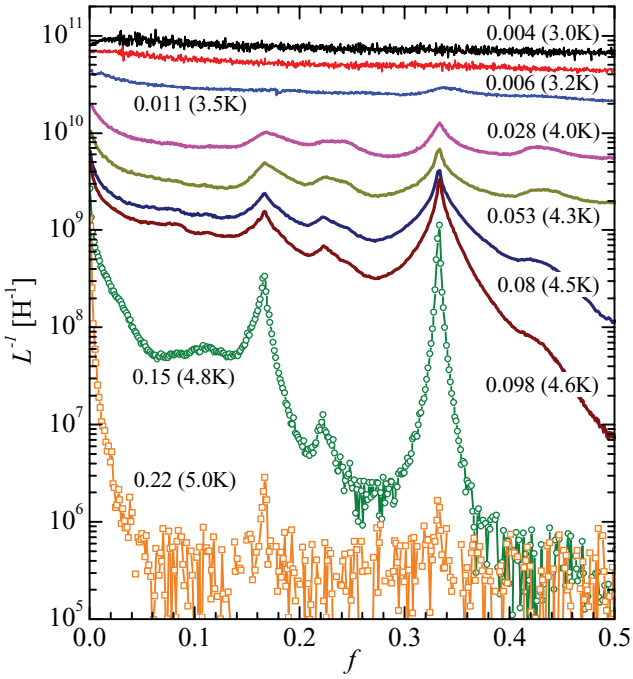

Fig. 2: (Colour on-line) Inverse magnetoinductance $L^{-1}(f)$ isotherms measured in the temperature range between $\tau=0.22$ ($T=5\,\mathrm{K}$) and $\tau=0.004$ ($T=3\,\mathrm{K}$) with an excitation frequency $\omega/2\pi=16\,\mathrm{Hz}$.

Well-defined structures are measured at low excitation frequency showing peaks in $L^{-1}(f)$ which reveal enhanced superconducting phase coherence for some rational values of frustration ($f=0,1/6,2/9,1/3$). The $f=1/3$ state has been the subject of previous work which shows that a strongly enhanced superconducting phase coherence, as for $f=1/3$, does not necessarily imply that the vortex pattern is ordered [16,17], even if ordering in the vortex pattern is normally associated with the commensurability between the vortex lattice induced by B and the array geometry, and resulting in a strong phase coherence as shown in fig. 2 for $f=1/3$. The fully frustrated state ($f=1/2$), which on the contrary shows a pronounced depressed response in the intermediate-temperature range, was also investigated [18,19] and for both the $f=1/3$ and $f=1/2$ states the magnetic interaction between screening currents circulating in neighbouring cells of the array has been considered, but still assuming a uniform frustration over the array. Starting from the hottest isotherms and lowering the temperature, $L^{-1}(f)$ first shows the appearance of well-defined structures at $f=0,1/6,1/3$ which grow up until some temperature $\tau\approx 0.1$. While further lowering the temperature the structures progressively disappear as shown by the coldest isotherms in fig. 2.

Clues about the very low-temperature response ($\tau<10^{-2}$) come from the temperature behaviour of the array penetration length. For a thin superconducting film of

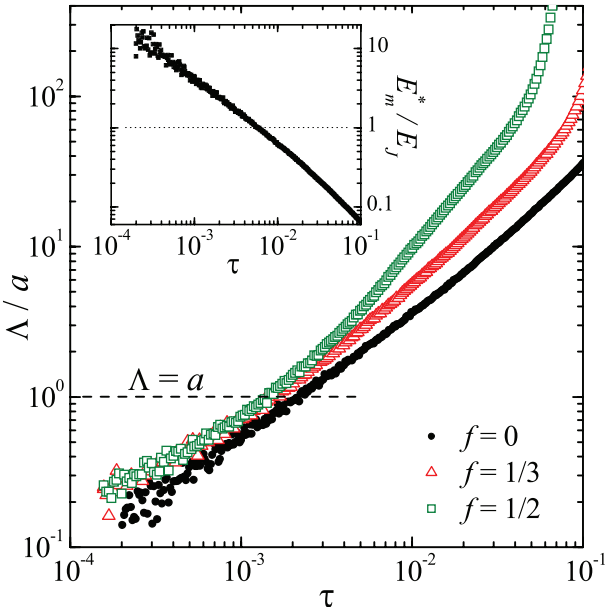

Fig. 3: (Colour on-line) Low-temperature dependence of the effective penetration length Λ in unit of the lattice parameter $a = 8\,\mu$m (see upper inset to fig. 1) for three frustration values $f = 0, 1/3, 1/2$. Inset: energy ratio $E^{\star}_m/E_J$ as a function of reduced temperature τ.

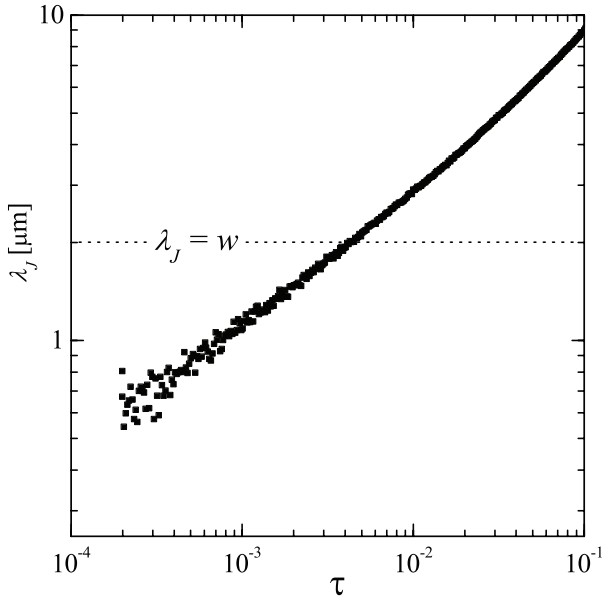

Fig. 4: Josephson penetration length λ_J as a function of reduced temperature τ. The dashed line indicates the size of a junction (width $w = 2\,\mu$m).

thickness d and exposed to B the screening distance is given by a thickness-dependent penetration length [20], the bulk material (3D) penetration depth λ being rescaled according to the thickness d, the effective 2D penetration length is $\Lambda = 2\lambda^2/d$. In the case of an array, Λ can be expressed in terms of I_c [12], or as mentioned above as a function of the measured sheet inductance; $\Lambda = 2(2/\sqrt{3})L/\mu_0$ for a *dice* lattice. Figure 3 shows the low-temperature dependence of Λ expressed in unit of the lattice parameter a for three values of frustration: $f = 0$, $f = 1/3$, and $f = 1/2$.

At very low temperature, below $\tau \approx 3 \cdot 10^{-3}$, the field dependence of Λ (*i.e.* the superconducting phase coherence) is suppressed in good agreement with the magnetoinductance isotherms of fig. 2. Most interestingly, this temperature is very close to the temperature at which $\Lambda = a$, the lattice parameter. In other words, for Λ close to or smaller than the lattice parameter the sample no longer behaves as a JJA with characteristic size a. This observation suggests the presence of strong magnetic screening. More information is obtained by comparing the magnetic energy E_m stored in each supercurrent I_s loop around the lattice plaquettes with the Josephson energy E_J. For the sake of simplicity E_m is overestimated by considering the maximum supercurrent, *i.e.* the critical current I_c; $E_m = \frac{1}{2}\mathcal{L}I_s^2 \leqslant \frac{1}{2}\mathcal{L}I_c^2 = E_m^*$. The geometrical inductance $\mathcal{L} = 26\,$pH of a rhombic loop (see upper inset to fig. 1) is calculated using the numerical results of [21] for a wire with rectangular cross-section. The ratio E_m^*/E_J shown in the inset of fig. 3 shows that the magnetic energy is dominating over the Josephson energy for temperatures $\tau < 5 \cdot 10^{-3}$.

Screening effects also appear locally on each Josephson junction, inside which Meissner screening fields are responsible for inhomogeneous distribution of the Josephson currents. Quantitatively this phenomenon is negligible for small junctions, *i.e.* when the junction width $w \ll \lambda_J$ the Josephson penetration length given by $\lambda_J = \sqrt{\hbar/(2e\mu_0 l J_c)}$ [22], where J_c is the cross-section critical current density and l is the junction length (see fig. 1). Figure 4 shows the temperature dependence of λ_J which is smaller than the junction width w for $\tau < 4 \cdot 10^{-3}$. Thus, at lower temperature the current distribution inside the junctions is no longer homogeneous. As a consequence, the phase difference across the junction width is no longer unique and the JJA cannot be mapped onto the XY model.

There exist two different mechanisms for the suppression of the magnetic-field dependence of the sheet inductance measured at finite frequency while the temperature is lowered: magnetic screening induced by superconducting currents in the array and the vanishing of thermal fluctuations leading to the freezing of the vortex diffusion between array cells. Evidence for the predominance of the first mechanism at the lowest temperatures comes from a comparison of the measured sheet inductance with the same quantity calculated in the XY regime and in the absence of thermal fluctuations, *i.e.* the ground-state value of $L^{-1}(f)$ calculated within the frustrated XY model at selected frustration states $f = 0, 1/3, 1/2$. At very low temperature where thermal fluctuations can be neglected, the JJA is equivalent to

a network of inductances [23] $L_{ij}(q_{ij})$ and the phase variables q_{ij} are known in the frustrated ground states at $f=1/3$ [17] and at $f=1/2$ [19]. Each ground state is characterised by a sheet inductance $L(f)$ that can be calculated from the frustrated inductance network L_{ij} which is first transformed into an anisotropic triangular lattice L'_{ij} by the triangle-star transformation [15]. $L(f)$ is then calculated applying Kirchhoff's laws to the elementary cell of the transformed network L'_{ij}.

Unfrustrated state $f=0$. – All bonds of the transformed triangular lattice have the same inductance value, hence the isotropic sheet inductance of the dice lattice $L(0)=(\sqrt{3}/2)L_J$ with L_J the single-junction inductance at zero field.

Frustrated state $f=1/3$. – Here we consider the (honeycomb) ground state which is dominating on a short scale over the possible vortex configurations [17]. The transformed sheet inductance is isotropic; $L(1/3)=(4\sqrt{3}/5)L_J\cong 1.39L_J$.

Fully frustrated state $f=1/2$. – Applying the triangle-star transformation to the four periodic ground states [19], we obtain two different configurations each with two inductance components. Thus, in the ground state of the fully frustrated XY model the JJA behaves as a two-component inductance network (L_x, L_y). Moreover, due to the inefficiency of the degeneracy removal mechanism and the prominence of the finite-size effects [19] the vortex pattern can be assumed as disordered. In a 2D disordered system with two phases equally distributed, the conductivity is given by the geometric mean of both phase conductivities [24]. Although in principle one should then consider the geometric mean of (L_x, L_y), the discussion on the choice of the mean value, *i.e.* the arithmetic or the geometric mean, is irrelevant since they are almost the same and the experimental resolution does not allow us to distinguish the two. The four periodic states [19] share the same geometric mean $L(1/2)=3\sqrt{3}/(2\sqrt{2})L_J\cong 1.84L_J$.

The calculated sheet inductances $L(f)$ are theoretical predictions based on the XY model in the absence of thermal fluctuations and so have to be compared with low-temperature data taken at high frequency where the corresponding time scale is too short to allow for fluctuations. Figure 5 shows ratios of $L^{-1}(f)$ extracted from low-temperature inverse magnetoinductance isotherms like those in fig. 2 but at much higher frequency $(\omega/2\pi=16\,\mathrm{kHz})$ and at $f=0,1/3,1/2$. The data in fig. 5 unambiguously demonstrate that at low temperature the modulation of the measured sheet inductance is weaker than it would be in the related XY model in the absence of thermal fluctuations, and the selected ratios tend to unity. This behaviour can definitively be ascribed to magnetic screening effects.

Conclusion. – The field modulation of the sheet inductance in Josephson-junction arrays on a *dice* lattice is shown to vanish while lowering the temperature.

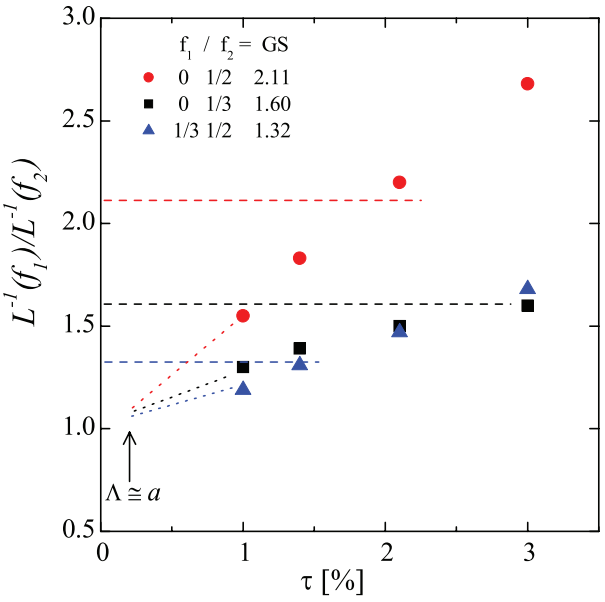

Fig. 5: (Colour on-line) Low-temperature sheet inductance ratios $L^{-1}(f_1)/L^{-1}(f_2)$ at selected frustration states $f_1, f_2 = 0, 1/3, 1/2$ extracted from high-frequency $(\omega/2\pi=16\,\mathrm{kHz})$ magnetoinductance isotherms. Horizontal (coloured) dashed lines show the values of the ratios calculated in the corresponding frustrated XY ground states (GS). The arrow indicates the temperature at which $\Lambda\cong a$ (extracted from fig. 3).

The response is field independent below a reduced temperature $\tau=k_BT/E_J\approx 10^{-3}$, or equivalently below an easily accessible temperature $T\approx 3\,\mathrm{K}$. Note that this threshold temperature may change in samples with substantially different geometrical parameters. The very low-temperature regime is characterised by a penetration length shorter than the lattice parameter, and the magnetic energy associated with screening currents is greater than the Josephson coupling energy. The observed behaviour is explained in terms of increasing magnetic screening, with decreasing temperature, until a strong screening regime is reached where the modulation of the measured sheet inductance is weaker than in the frustrated XY model in the absence of thermal fluctuations. The disappearance of the modulation in the magnetoinductance at low-temperature could also be attributed to vortices with very low mobility. However, this would give rise to a hysteretic response that was not observed down to the lowest accessible temperatures. In the (very) low-temperature screening regime, the JJA behaves as a multiply connected superconductor, and the XY model is no longer valid. Unlike the weak-screening regime where vortices are phase configurations satisfying the fluxoid quantisation, in this strong-screening regime vortices are real magnetic objects carrying an integer number of flux quanta and interacting with currents through Lorentz forces. These strong effects highlight the importance of a careful interpretation of low-temperature results within the frustrated XY model.

* * *

MT is grateful to V. I. Marconi for critical reading of the manuscript. The data presented in this paper were taken when both authors were working in the group of P. Martinoli at the University of Neuchâtel (Switzerland) and we appreciated his comments and suggestions. This work was supported by the Swiss National Science Foundation.

REFERENCES

[1] Teitel S. and Jayaprakash C., *Phys. Rev. Lett.*, **51** (1983) 1999; Halsey T. C., *Phys. Rev. B*, **31** (1985) 5728.
[2] Martinoli P. and Leemann Ch., *J. Low Temp. Phys.*, **118** (2000) 699; Newrock R. S. *et al.*, *Solid State Phys.*, **54** (2000) 263.
[3] Fazio R. and van der Zant H., *Phys. Rep.*, **355** (2001) 235.
[4] Stroud D. and Kivelson S., *Phys. Rev. B*, **35** (1987) 3478; Petraglia A., Filatrella G. and Rotoli G., *Phys. Rev. B*, **53** (1996) 2732.
[5] Domínguez D. and José J. V., *Phys. Rev. B*, **53** (1996) 11692.
[6] Majhofer A., Wolf T. and Dietrich W., *Phys. Rev. B*, **44** (1991) 9634; Domínguez D. and José J. V., *Phys. Rev. Lett.*, **69** (1992) 514; Phillips J. R. *et al.*, *Phys. Rev. B*, **47** (1993) 5219.
[7] Jeanneret B. *et al.*, *Appl. Phys. Lett.*, **55** (1989) 2336.
[8] Meyer R. *et al.*, *Phys. Rev. Lett.*, **67** (1991) 3022.
[9] Rüfenacht A. *et al.*, *Phys. Rev. Lett.*, **96** (2006) 227002.
[10] Lobb C. J., Abraham D. W. and Tinkham M., *Phys. Rev. B*, **27** (1983) 150.
[11] Tesei M., PhD Thesis, University of Neuchâtel-Switzerland (2005).
[12] Tinkham M., *Introduction to Superconductivity*, second edition (McGraw-Hill, New York) 1996.
[13] Wilhelm F. K., Zaikin A. D. and Schön G., *J. Low Temp. Phys.*, **106** (1997) 305.
[14] Rzchowski M. S. *et al.*, *Phys. Rev. B*, **42** (1990) 2041; Benz S. P. *et al.*, *Phys. Rev. B*, **42** (1990) 6165.
[15] Korshunov S. E., Meyer R. and Martinoli P., *Phys. Rev. B*, **51** (1995) 5914.
[16] Serret E., Butaud P. and Pannetier B., *Europhys. Lett.*, **59** (2002) 225.
[17] Korshunov S. E., *Phys. Rev. Lett.*, **94** (2005) 087001.
[18] Pannetier B. *et al.*, *Physica C*, **352** (2001) 41; Tesei M., Théron R. and Martinoli P., *Physica C*, **437** (2006) 328.
[19] Korshunov S. E., *Phys. Rev. B*, **63** (2001) 134503; **71** (2005) 174501.
[20] Pearl J., *Appl. Phys. Lett.*, **5** (1964) 65.
[21] Grover F. W., *Inductance Calculations, Dover Phoenix Editions Series* (Dover Publications) 2004, ISBN-13: 9780486495774.
[22] Barone A. and Paterno G., *Physics and Applications of the Josephson Effect* (John Wiley, New York) 1982.
[23] Yu W. and Stroud D., *Phys. Rev. B*, **50** (1994) 13632.
[24] Dykhne A. M., *Zh. Eksp. Teor. Fiz.*, **59** (1970) 110; *Sov. Phys. JETP*, **32** (1971) 63.